A NEW RIG FOR THE MEASUREMENT OF ROTARY AND TRANSLATIONAL DERIVATIVES

by

C.O. O'Leary, B. Weir, J.M.Walker
Defence Research Agency, Bedford, United Kingdom

Abstract

An important contribution to the study of flight characteristics of combat aircraft is dynamic testing in wind tunnels. One type of test is the measurement of aerodynamic derivatives using a small-amplitude oscillatory rig. In addition to providing essential information about the stability of an aircraft, these parameters are used in mathematical models and simulators to predict flight response. For many years oscillatory tests have been made at DRA using an apparatus known as the Flexible Sting Rig (FSR). This rig is limited in some respects and it was decided to construct a new rig with a rigid sting and inexorable motion.
The present paper describes the design and testing of a five degree-of-freedom (pitch, heave, yaw, sway and roll) rig and discusses results from tests on a canard-configured research model. Effects of model configuration and frequency of oscillation were investigated and results are compared with those from oscillatory tests with the FSR. Measurements of cross-coupling derivatives and derivatives due to $\dot{\alpha}$ and $\dot{\beta}$ (acceleration derivatives) are included.

List of Symbols

b	wing span, m
c	aerodynamic mean chord
C_l	rolling moment / q S b
C_m	pitching moment / q S c
C_n	yawing moment / q S b
LVDT	Linear Variable Differential Transducer
q	dynamic pressure, N/m^2
q	rate of pitch
r	rate of yaw
v	velocity component along y axis
V	wind velocity
w	velocity component along z axis
α	angle-of-attack, rad or deg
$\dot{\alpha}$	rate of change of angle of attack
β	angle-of-sideslip, rad or deg
$\dot{\beta}$	rate of change of angle of sideslip
ω	circular frequency, rad/sec
Ω_b	frequency parameter for yaw, sway and roll tests, $\omega b/2V$
Ω_c	frequency parameter for pitch and plunge tests, $\omega c/2V$

Derivatives:

$C_{l\beta} = \partial C_l/\partial\beta$

$C_{m\alpha} = \partial C_m/\partial\alpha$

$C_{n\beta} = \partial C_n/\partial\beta$

$C_{l\dot{\beta}} = \partial C_l/\partial(\dot{\beta}b/2V)$

$C_{m\dot{\alpha}} = \partial C_m/\partial(\dot{\alpha}c/2V)$

$C_{n\dot{\beta}} = \partial C_n/\partial(\dot{\beta}b/2V)$

$C_{lp} = \partial C_l/\partial(pb/2V)$

$C_{lr} = \partial C_l/\partial(rb/2V)$

$C_{lq} = \partial C_l/\partial(qc/2V)$

$C_{mq} = \partial C_m/\partial(qc/2V)$

$C_{mr} = \partial C_m/\partial(rb/2V)$

$C_{nq} = \partial C_n/\partial(qc/2V)$

$C_{nr} = \partial C_n/\partial(rb/2V)$

Introduction

An important contribution to the study of flight characteristics of combat aircraft is dynamic testing in wind tunnels. One type of test is the measurement of aerodynamic derivatives

using a small-amplitude oscillatory rig. In addition to providing essential information about the stability of an aircraft, these parameters are used in mathematical models and simulators to predict flight response. The application of derivatives is, strictly speaking, limited to small perturbations from steady flight and should not generally be applied to the prediction of large amplitude motion at high angles-of-attack. For prediction of manoeuvring flight characteristics where forces and moments may depend on the history of the motion and where there are large amplitude and frequency effects, the flight manoeuvre should, ideally, be represented in the wind tunnel. Since this is difficult to achieve in practice, investigation and prediction of high alpha manoeuvring flight characteristics relies on a combination of theoretical methods and static and dynamic wind-tunnel test techniques which include small-amplitude oscillatory tests. Work on the DRA High Incidence Research Models showed how this approach could be successful in furthering the understanding of high angle-of-attack aerodynamics[1,2].

At DRA Bedford many small-amplitude oscillatory tests have been made with an apparatus known as the Flexible Sting Rig (FSR)[3]. With this rig the model is mounted on a flexible sting/balance and oscillated in various modes by 'tuning in' the appropriate natural frequency which is determined by the model inertia and balance stiffness, neither of which can be varied easily. Tests are made at the mode natural frequencies only. The model reacts to aerodynamic forces, so model response is measured and equations of motion are solved for in-phase and in-quadrature components of the balance signals to extract the desired derivatives. However at high angles-of-attack, where there is separated flow over the model, motion becomes erratic and accuracy of measurement is degraded. Thus the FSR cannot be used for investigation of effects of frequency and is not entirely satisfactory for tests at high angle-of-attack. Another disadvantage of the FSR is that, due to relatively high mass and inertia of the model, it is not possible to measure derivatives due to $\dot{\alpha}$ and $\dot{\beta}$, (e.g. $C_{m\dot{\alpha}}, C_{n\dot{\beta}}$.) with acceptable accuracy. These are equivalent in the first approximation to derivatives due to translational acceleration in the same plane of motion ($\dot{\alpha} = \dot{w}/V$, $\dot{\beta} = \dot{v}/V$).

An alternative test technique is to oscillate the model on a 'rigid' sting, where motion is assumed to be inexorable. In this case the model is mounted on a stiff balance and the sting is driven by a variable frequency power source through an inflexible mechanical linkage. It is assumed that the motion of the model is determined by the drive alone and aerodynamic loads have no effect on the motion. With such a rig frequency effects can be investigated and high angle-of-attack test data should be more accurate. Disadvantages of this technique are:

a. Inexorable motion requires relatively high power, which generally occupies a large volume and may create unacceptable blockage if placed in the airstream.
b. To obtain acceptable accuracy and to eliminate deflections of the model due to inertial and aerodynamic loads it is necessary to test a very light model on a stiff but sensitive balance. The wind-tunnel support must be very rigid. Test speeds may be limited because of model and balance strength limitations.

With conventional steel/aluminium alloy/glass fibre wind-tunnel models of span 1.2 m and mass 60 kg it was difficult to satisfy these requirements and the FSR type of rig has been preferred. However, in recent years it has been possible to construct similar size models with a mass of only 6 kg but strong enough for low speed testing. A drive mechanism and balance could be designed and mounted on an existing dynamic test support structure in the 13ft x 9ft low speed wind tunnel at DRA Bedford. Such a rig could be designed to measure both rotary and translational motion derivatives in longitudinal and lateral tests.

The first rig constructed was limited to translational (plunge and sway) motion and applied to the measurement of acceleration derivatives[4]. The present paper describes the design and testing of a five degree-of-freedom (pitch, heave, yaw, sway and roll) rig and discusses results from tests on a canard-configured research model. Effects of model configuration and frequency of oscillation were investigated and results are compared with those from oscillatory tests with the FSR. Measurements of cross-coupling and acceleration derivatives are included.

Description of rig and data acquisition system

The main component of the rig, shown in Fig 1, is a model support sting which can be oscillated in five degrees of freedom, i.e. pitch, plunge (heave), yaw, sway and roll. The rig is shown configured for the plunge mode in Fig 1a and the pitch mode in Fig 1b. For sway and yaw the sting and swinging arm assembly are fitted at 90° to that shown. The flared downstream end of the sting is mounted on the swinging arm assembly which converts a rotational shaft drive on the wind-tunnel axis to oscillatory harmonic motion using a 'scotch yoke' slider-in-slot mechanism. The sleeve mounting for the swinging arms fits over the shaft housing and the base plate is bolted to the support structure in either of the two positions. Amplitude of the motion is varied by adjusting the throw of the slider within a limit of ±50 mm. The slot is aligned horizontally for pitch and heave motion and vertically for yaw and sway motion. Change of alignment is accomplished by rotating the assembly through 90°. For translational motion, i.e. heave and sway , the swinging arms are parallel. For pitch and yaw motion the rear stationary pivots of the swinging arms are moved further apart as shown in Fig 1b. The centre of oscillation coincides with the balance axis. Frequency of oscillation is dependent on shaft speed which is controlled by a servo valve. For the roll mode the motor shaft drives the sting directly with the motor controlled by the servo valve and closed-loop control system gives the required oscillatory motion about the sting axis. Forces acting on the model are measured by a strain gauge balance which is integral to the sting.

A hydraulic power pack, situated outside the wind-tunnel working section supplies the motor with fluid at 1500 psi pressure via a rigid pipe and swivel joint linkage. The whole assembly is mounted on a carriage which is traversed along the twin support quadrants to vary angle-of-attack up to a limit of 42°. For all modes, except roll, model motion is measured with an accelerometer in the model, linear for heave and sway tests and angular for pitch and yaw tests. These accelerometer signals are also used to cancel inertial loadings on the strain gauge balance. The sensitive axes of the accelerometers are re-aligned in the appropriate direction for each type of test. For the rolling mode, motion is measured with a displacement transducer (LVDT).

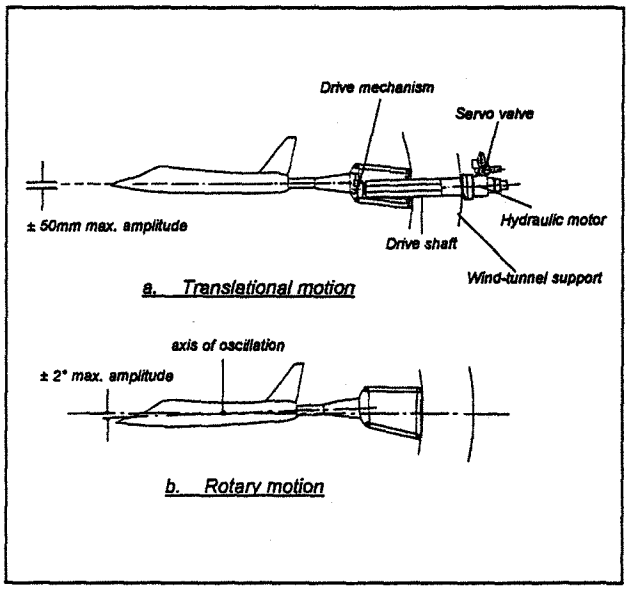

Fig 1. General Arrangement of Inexorable Rig

The data acquisition system consists of a signal processing unit, A-to-D converter and Fourier Transform software on a Masscomp computer. Strain gauge balance signals and the accelerometer or LVDT signal are amplified and filtered using matched 20Hz filters. In addition, phase lags are introduced in the strain gauge signals so as to match the accelerometer or LVDT signal to better than 0.2° over the frequency range of the tests. Interactions are eliminated within a signal mixing unit. After conversion to digital form the in-phase and in-quadrature components of the signals are determined using a discrete Fourier Transform and the components are normalised with respect to the reference accelerometer or LVDT signal. After testing, the data is downloaded onto a PC for post-test data reduction and analysis.

Description of model

A general arrangement and principal dimensions of the HIRM 2 model are shown in Fig 2. HIRM 2 is a close-coupled delta-canard 'agile fighter' configuration with a wing leading edge sweep of 58°. The wing is optimised for high subsonic speed manoeuvring flight with a leading edge droop of 12.5°. The fuselage is square sectioned with

rounded corners and blends into a circular section nose forward of the foreplanes. Foreplanes and fin have thin symmetrical sections. For the present tests the model was fitted with a short nose boom. All tests were made transition free.

The model is manufactured from lightweight materials, principally a close-cell foam with an external skin consisting of a fibre glass 'scrim' of thickness varying between 0.2 mm and 0.4 mm. The balance housing is a thin-walled aluminium tube. Total model mass is less than 6 kg and the normal force limit is 750 N.

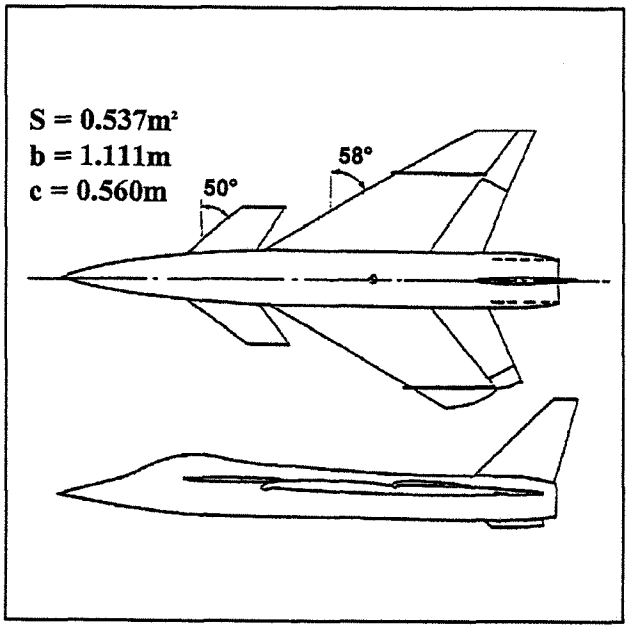

Fig 2. General Arrangement of HIRM 2

Method of test and data reduction

Prior to wind-on testing the LVDT, linear and angular accelerometers and the strain gauge balance were calibrated and first order balance interactions removed by means of a signal mixing unit. With the model mounted on the balance, for all modes except roll, signals due to inertial loading were cancelled, wind-off, at the required test frequencies using the accelerometer tare controls on the mixing unit. For wind-on tests, at the desired frequencies and amplitudes, the measurements were further corrected by subtracting residual wind-off signals at the same frequency and amplitude. For the pitch, heave, yaw and sway modes the amplitude was set by adjusting the throw on the slider and frequency was set by adjusting the speed of the hydraulic motor. For roll tests frequency and amplitude were set on the electronic control system.

Wind speeds, limited by the strength of the balance, were 25 m/s for pitch and heave tests and 30 m/s for yaw, sway and roll. Reynolds number, based on aerodynamic mean chord, was approximately one million. Angle-of-attack range was 0° to 42° and all tests were made at zero mean sway angle. Owing to the form of the rig support structure it was not possible to test at non-zero mean sway angle without inducing an unacceptable sidewash on the model. No attempt was made to include still air damping or 'virtual inertia' by shrouding the model for the wind-off tests. This may be possible in future testing by enclosing the model in a light plywood or fibre glass enclosure fixed to earth.

The on-line data acquisition system resolves the strain gauge balance signals into in-phase and in-quadrature components which are normalised with respect to the accelerometer or LVDT signal depending on the mode of oscillation. These components were converted to stiffness and damping derivatives in body axes using the appropriate calibration factors, model and wind constants. The reference axis of the model is coincident with the balance axis so no axis shift was required.

Results and discussion

Results are presented in the form of longitudinal and lateral body axes derivatives which are defined in the List of Symbols. In rotary tests derivatives due to q, p and r are measured in combination with those due to $\dot{\alpha}$ and $\dot{\beta}$, e.g. $(C_{mq} + C_{m\dot{\alpha}})$. Frequency is non-dimensionalised with respect to c for longitudinal data and b for lateral data, i.e. $\Omega_c = \omega c/2V$ and $\Omega_b = \omega b/2V$.

Effects of frequency

Effects on $C_{m\alpha}$, $C_{n\beta}$ and $C_{l\beta}$

Effects of frequency on the 'static' derivatives: gradient of pitching moment, $C_{m\alpha}$, directional stability, $C_{n\beta}$, and rolling moment due to sideslip, $C_{l\beta}$ are shown in Figs 3 & 4. These measurements were obtained from in-quadrature components in translational tests where the amplitude

of oscillation was ± 50 mm, corresponding to perturbation amplitudes in α and β of ± 1.5° and ± 3° for the two test frequencies of 2 Hz and 4 Hz respectively. Previous tests[4] indicated that this difference in perturbation amplitude was not significant.

For virtually all test angles-of-attack, $C_{m\alpha}$ (Fig. 3) is more positive, i.e. less stable, with increase in frequency but the sharp reversals in gradient are less evident at the higher frequency ; the positive 'spike' at α = 19° is evident for Ω_c = 0.14 but not for Ω_c = 0.28. Apparently, the aerodynamic feature which caused the spike is sensitive to frequency parameter, i.e. the ratio of oscillation frequency to chord lengths of air passing the model in unit time. Effects of frequency on the directional and lateral derivatives, $C_{n\beta}$ and $C_{l\beta}$, are also significant. Up to α = 30°, directional stability $C_{n\beta}$ (Fig 4) decreases with increasing frequency, approximately 40 % at α = 0°. When the model was tested with fin off (not presented) there was negligible frequency effect on $C_{n\beta}$ at low α, indicating that increasing frequency reduces fin effectiveness. Early NASA dynamic tests[5] on a 60° delta model showed that $C_{n\beta}$ was at a maximum for $\Omega_b \approx 0.12$. The lateral stability derivative $C_{l\beta}$ (Fig. 4) is not affected by frequency at low angle-of-attack but for α > 28° there is a much greater loss in stability, i.e more positive, at low frequency. Similar results were noted in the NASA work.

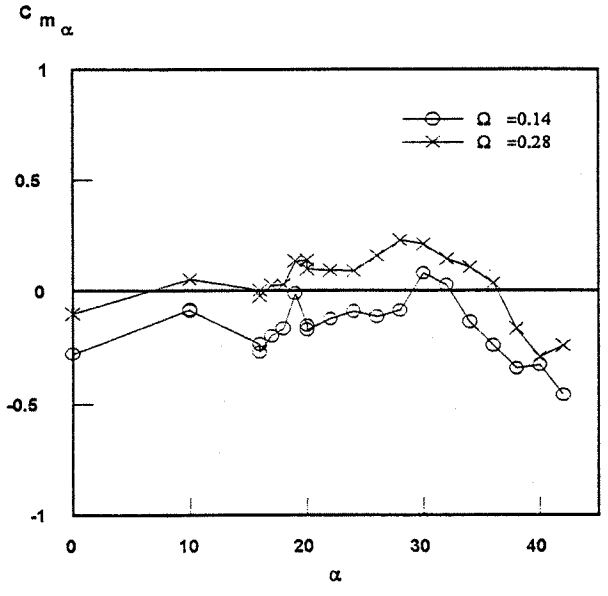

Fig 3. Effect of frequency on $C_{m\alpha}$ from plunging motion

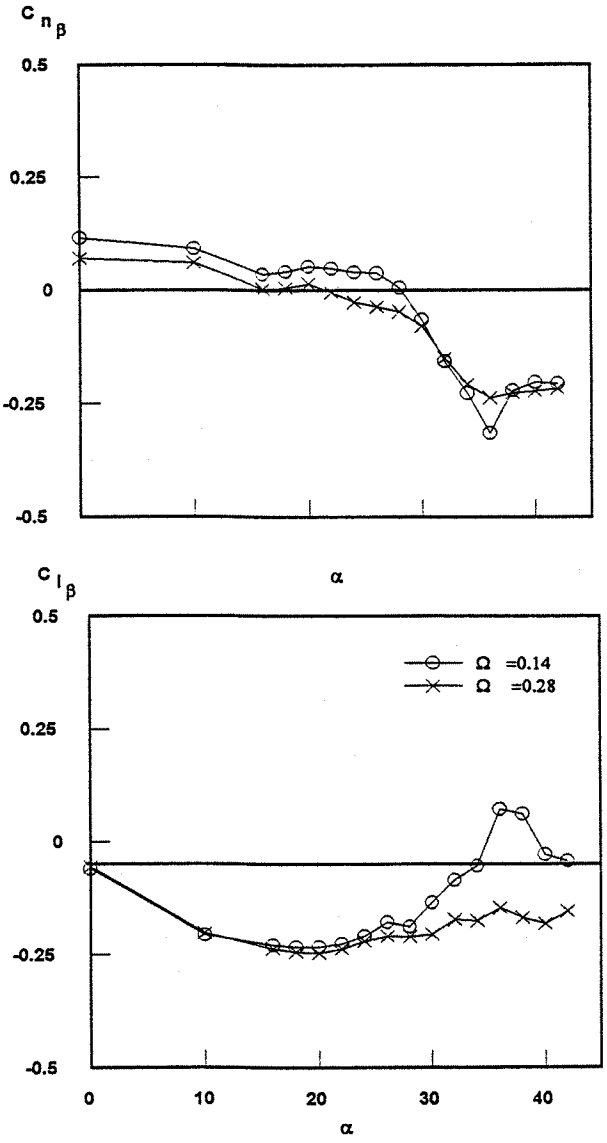

Fig 4. Effect of frequency on $C_{n\beta}$ and $C_{l\beta}$ from sway mode

Effects on dynamic derivatives

Effects of frequency on pitching moment derivatives $C_{m\dot{\alpha}}$ and $(C_{mq} + C_{m\dot{\alpha}})$ is shown in Fig 5. The acceleration derivative $C_{m\dot{\alpha}}$ was measured in plunging motion as an in-phase signal, whereas the combined derivative $(C_{mq} + C_{m\dot{\alpha}})$ was measured in pitching motion as an in-quadrature signal. The results indicate that at low angle-of-attack $C_{m\dot{\alpha}}$ is about one third the magnitude of C_{mq} but of the opposite sign (de-stabilising). In both cases there is a positive spike at the lower frequency, at $\alpha \approx 19°$, as in the case of $C_{m\alpha}$. Both derivatives are also more negative at high angle-of-attack at the lower frequency. The magnitude of $C_{m\dot{\alpha}}$ depends on the lag in

the development of lift over the foreplane and wing as angle-of-attack varies and the results show that this effect is reduced as frequency is increased. As will be shown later the spike is due to the foreplane or a foreplane/wing interaction and is eliminated at the higher frequency.

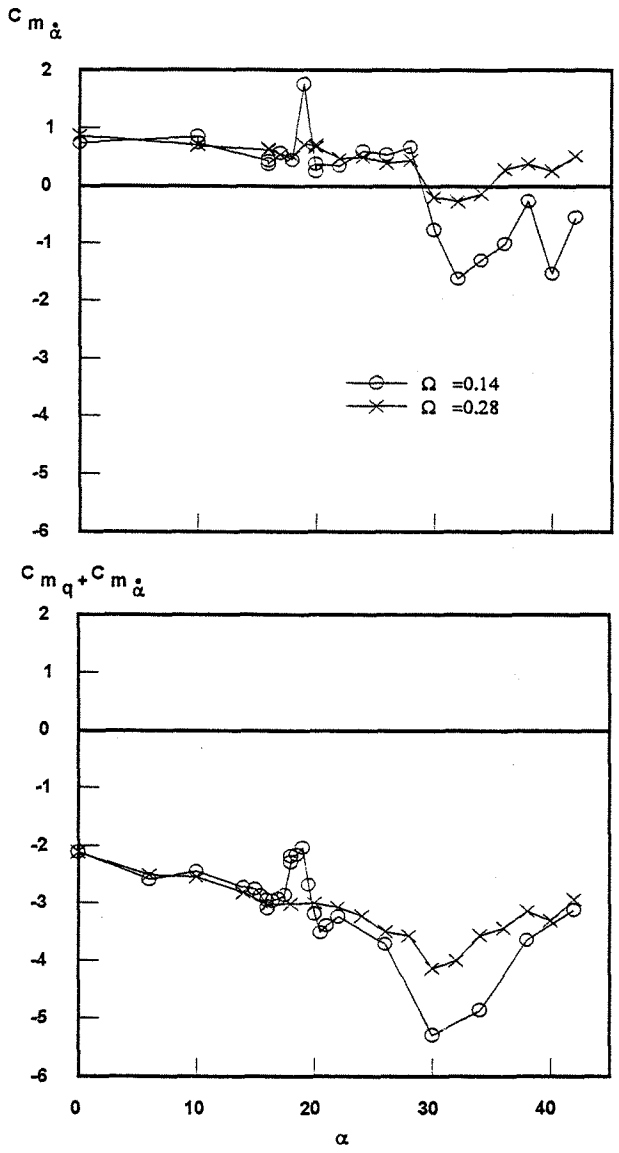

Fig 5. Effect of frequency on $C_{m\dot{\alpha}}$ and $(C_{mq}+C_{m\dot{\alpha}})$

Dynamic yawing moment derivatives obtained from sway, yaw and roll modes are shown in Fig 6. The acceleration derivative $C_{n\dot{\beta}}$, measured in the sway mode as an in-phase signal, is small at low angle-of-attack but, for Ω_b = 0.23, increases rapidly as angle-of-attack increases beyond 25°, At the higher frequency there is a much smaller increment at high angle-of-attack. It is probable that there are two main contributions to the $\dot{\beta}$

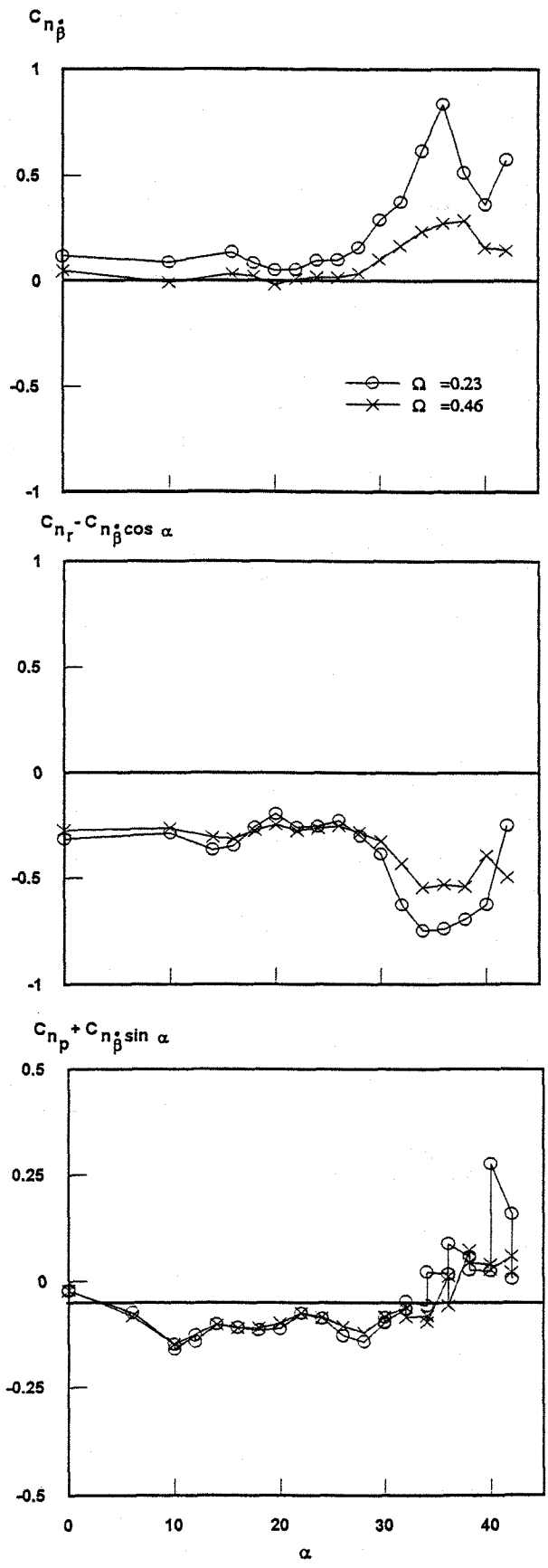

Fig 6. Effect of frequency on $C_{n\dot{\beta}}$, $(C_{nr}-C_{n\dot{\beta}}\cos\alpha)$ & $(C_{np}+C_{n\dot{\beta}}\sin\alpha)$

derivatives: firstly there is a lag in the vortical flow over the wings due to $\dot{\beta}$ and secondly, there is a lag in sidewash at the fin. It is probable that the latter has most effect on $C_{n\dot{\beta}}$, as discussed in the next section. These effects of frequency on $C_{n\dot{\beta}}$ are also apparent in the variation of the combined derivative $(C_{nr} - C_{n\dot{\beta}} \cos \alpha)$, where increases at high angle-of-attack are mainly accounted for by increases in the component due to $\dot{\beta}$. This derivative was measured in the yawing mode as an in-quadrature signal. There is, however, no apparent frequency effect on the cross derivative $(C_{np} + C_{n\dot{\beta}} \sin\alpha)$ measured in the roll mode. Repeatability of data is good except at the highest test angles-of-attack at the lower frequency.

The effects of frequency on three rolling moment derivatives: the acceleration derivative $C_{l\dot{\beta}}$, the damping-in-roll $(C_{lp} + C_{l\dot{\beta}} \sin \alpha)$ and the cross damping $(C_{lr} - C_{l\dot{\beta}} \cos \alpha)$ are shown in Fig 7. The lag in spanwise vortical flow across the wings due to $\dot{\beta}$ is the probable cause of the large increase in $C_{l\dot{\beta}}$ for $\alpha > 28°$, $\Omega_b = 0.23$.

As for $C_{n\dot{\beta}}$, increase in frequency diminishes the effect of $\dot{\beta}$, as was also found in previous work[5] at similar frequency parameters. Damping-in-roll is unaffected by frequency for $\alpha < 28°$ but thereafter increases in magnitude at the lower frequency only. Where there was more likely to be scatter in the measurements due to separated flow on the model data points were repeated for $30° < \alpha < 38°$. Measurements of $(C_{lp} + C_{l\dot{\beta}} \sin \alpha)$ indicate that the scatter is within 10%. At low/moderate angle-of-attack, the primary contribution to the cross-damping derivative $(C_{lr} - C_{l\dot{\beta}} \cos\alpha)$ is differential lift due to yawing and is a function of lift coefficient. For $\alpha > 28°$, $\Omega_b = 0.233$, there is a large increase in magnitude which is probably due, in large part, to the $C_{l\dot{\beta}}$ component. However, the sharp reduction at $\alpha = 36°$ is not evident in $C_{l\dot{\beta}}$. A similar frequency effect on this cross-damping derivative was found during NASA tests[6] on another fighter configuration.

Effects of model configuration

These effects were more evident at the lower test frequency and results are presented for the effects of foreplanes and the effects of fin at $\Omega_c = 0.14$ and $\Omega_b = 0.233$ respectively.
The effects of foreplanes on the

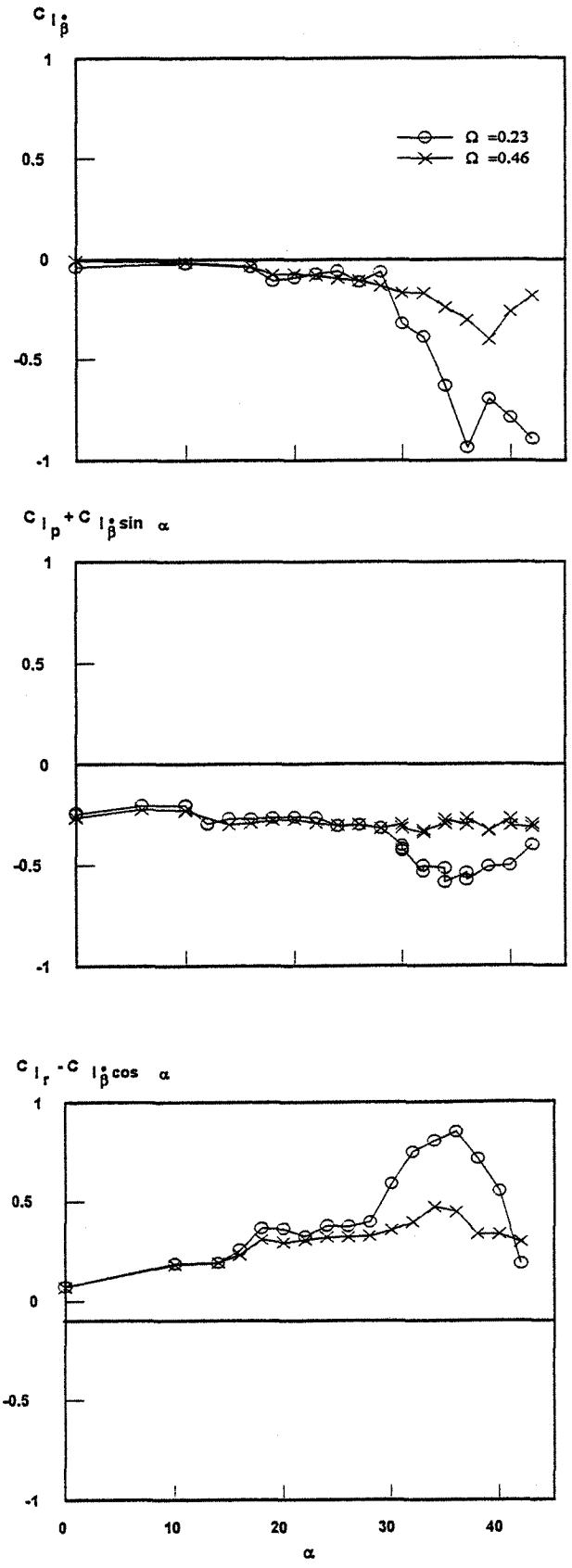

Fig 7. Effect of frequency on $C_{l\dot{\beta}}$, $(C_{lp}+C_{l\dot{\beta}}\sin\alpha)$ & $(C_{lr}-C_{l\dot{\beta}}\cos\alpha)$

acceleration derivative $C_{m\dot{\alpha}}$ and the pitch damping derivative $(C_{mq} + C_{m\dot{\alpha}})$ are shown in Fig 8. At low angle-of-attack $C_{m\dot{\alpha}}$ is unaffected by the presence of the foreplane but for $\alpha > 10°$ the presence of the foreplane has a marked effect on the variation with angle-of-attack. At $\alpha \approx 19°$ a positive increment of approximately 1.5 is only present with foreplanes on and is probably a flow lag interaction effect between the foreplane and the wing. As shown in Fig. 5, this interaction is sensitive to frequency parameter. At the highest test angles-of-attack, $\alpha > 35°$, foreplanes reduce the negative trend in $C_{m\dot{\alpha}}$. A comparison of the variation of $C_{m\dot{\alpha}}$ and $(C_{mq} + C_{m\dot{\alpha}})$ with angle-of-attack suggests that most of the variation is due to $C_{m\dot{\alpha}}$ and C_{mq} is substantially constant at around -3.

The foreplane interaction effect on the $C_{m\dot{\alpha}}$ component is again evident in the combined derivative measured in the pitching mode, agreeing with the plunging mode measurement of $C_{m\dot{\alpha}}$.

The contribution of the fin to the acceleration derivative $C_{n\dot{\beta}}$, and the combined derivative $(C_{nr} - C_{n\dot{\beta}} \cos \alpha)$, is shown in Fig 9. The fin makes a major contribution to $C_{n\dot{\beta}}$. There is a small positive increment at low angle-of-attack but for $\alpha > 25°$ there is a large increase in $C_{n\dot{\beta}}$ due to the fin. As may be expected the fin increases the magnitude of $(C_{nr} - C_{n\dot{\beta}} \cos \alpha)$. At low and moderate angle-of-attack the fin contributes to both components but for $\alpha > 25°$ the increase in magnitude is largely due to the fin contribution to $C_{n\dot{\beta}}$. These results suggest that the lag of sidewash over the fin is the source of the large increases in the magnitude of these derivatives at high angle-of-attack.

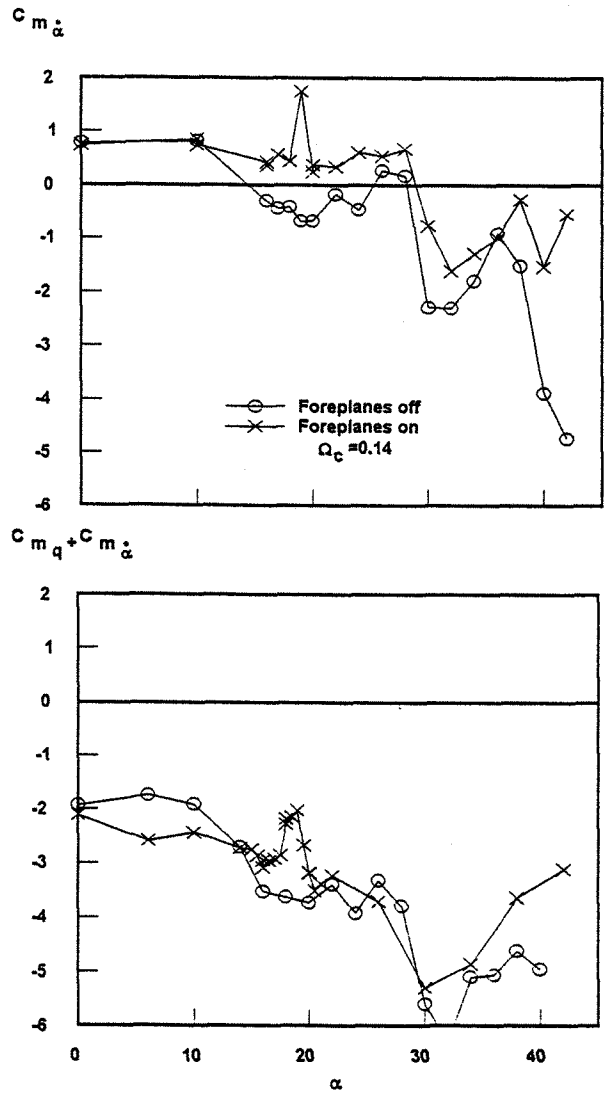

Fig 8. Effect of foreplanes on $C_{m\dot{\alpha}}$ and $(C_{mq}+C_{m\dot{\alpha}})$

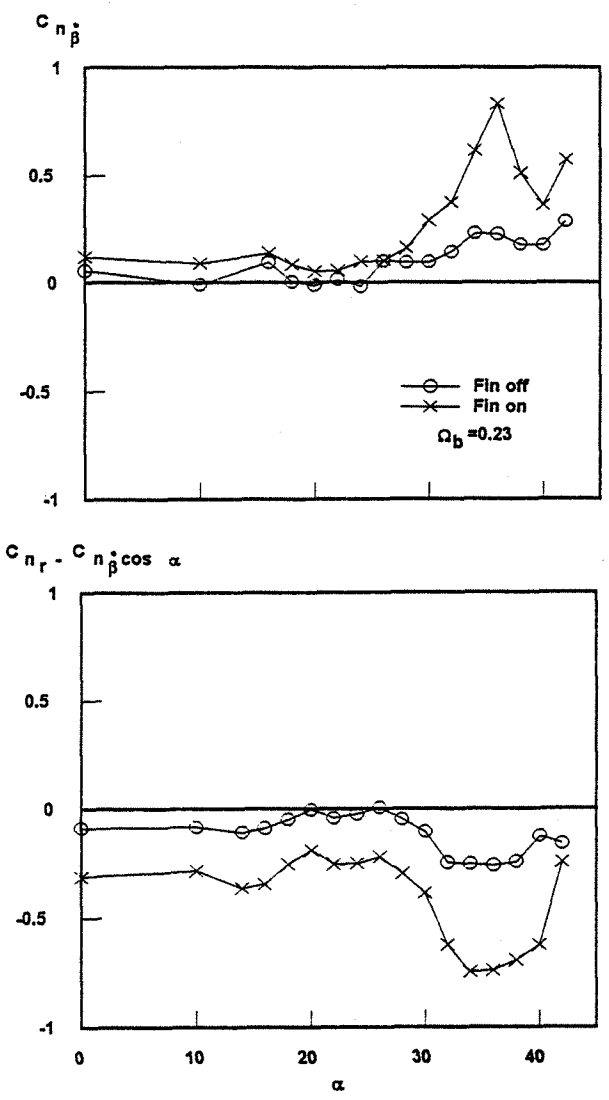

Fig 9. Effect of fin on $C_{n\dot{\beta}}$ and $(C_{nr}-C_{n\dot{\beta}}\cos\alpha)$

Rotational and translational mode measurements of 'static' derivatives

So called static or stiffness derivatives such as $C_{m\alpha}$, the gradient of pitching moment with angle-of-attack or $C_{n\beta}$, the gradient of yawing moment with angle-of-sideslip are obtained from both rotational and translational modes. $C_{m\alpha}$ is measured as an in-phase signal in the pitching mode and as an in-quadrature signal in the plunging mode. Similarly, $C_{n\beta}$ is measured as an in-phase signal in the yawing mode and as an in-quadrature signal in the sway mode. Measurements of $C_{m\alpha}$, $C_{n\beta}$ and $C_{l\beta}$ at the lower frequency are compared in Figs. 10 & 11. Although there are some detail differences in the variation with angle-of-attack there is generally good agreement between the in-phase and in-quadrature measurements. The most noticeable difference is in the high angle-of-attack variation of $C_{l\beta}$. Results from the sway mode show a positive increment of about 0.3 between α = 25° and α = 35° whereas results from the yawing mode show an increment of less than 0.1 in this range of angle-of-attack. It is interesting to note that sway mode results for the higher frequency shown in Fig 4 agree more closely with yawing mode results at the lower frequency in Fig 11. Results shown here and in earlier work[7] indicate that the magnitude of $C_{l\beta}$ at high angle-of-attack is particularly sensitive to dynamic effect, i.e. it depends on whether the test is static or dynamic and also on the frequency parameter and the mode of oscillation.

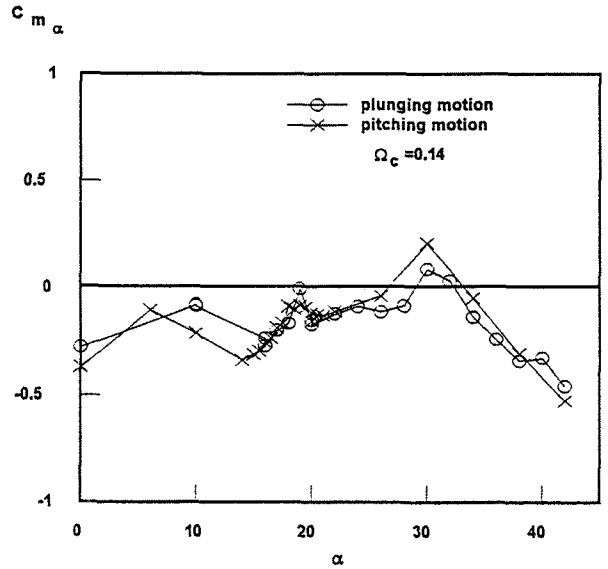

Fig 10. Comparison of $C_{m\alpha}$ for plunging and pitching motions

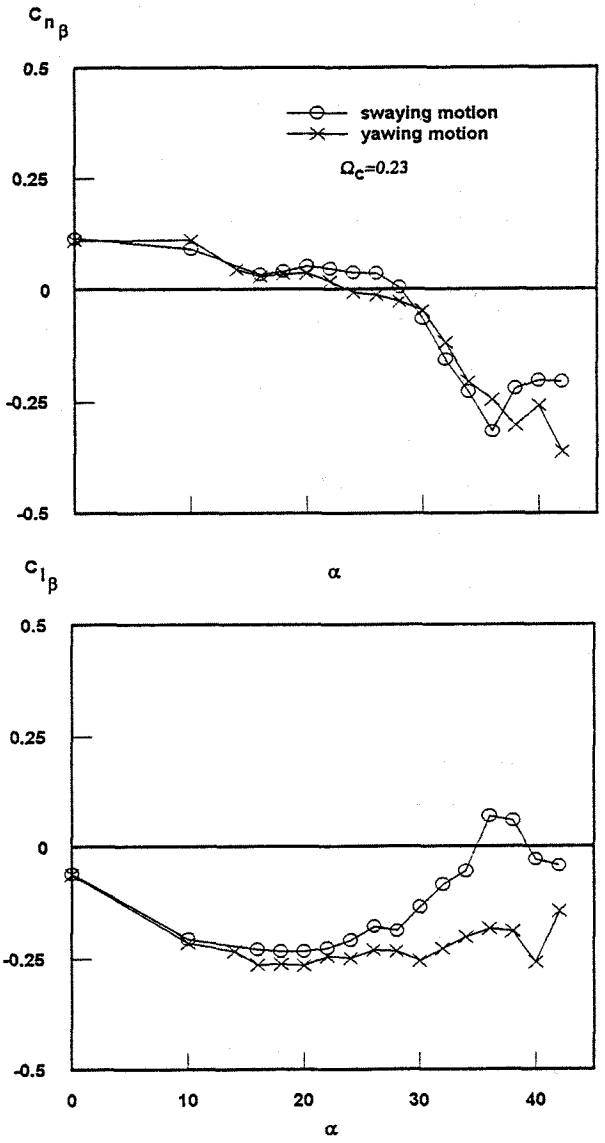

Fig 11. Comparison of $C_{n\beta}$ & $C_{l\beta}$ measurements from sway & yaw motions

The source of this derivative is differential wing lift due to sideslip and at high angle-of-attack the onset and nature of the flow separation will be sensitive to these factors.

Cross-coupling derivatives

Three cross-coupling derivatives, i.e. those coupling lateral forces with longitudinal motion and vice versa, $(C_{nq} + C_{n\dot{\alpha}})$, $(C_{lq} + C_{l\dot{\alpha}})$ and $(C_{mr} - C_{m\dot{\beta}} \cos \alpha)$ are shown in Figs 12 & 13. The magnitude of these derivatives is small for $\alpha < 25°$. At higher angles-of-attack there is an increase in the rolling moment derivative $(C_{lq} + C_{l\dot{\alpha}})$ which is then about 50% of the roll damping

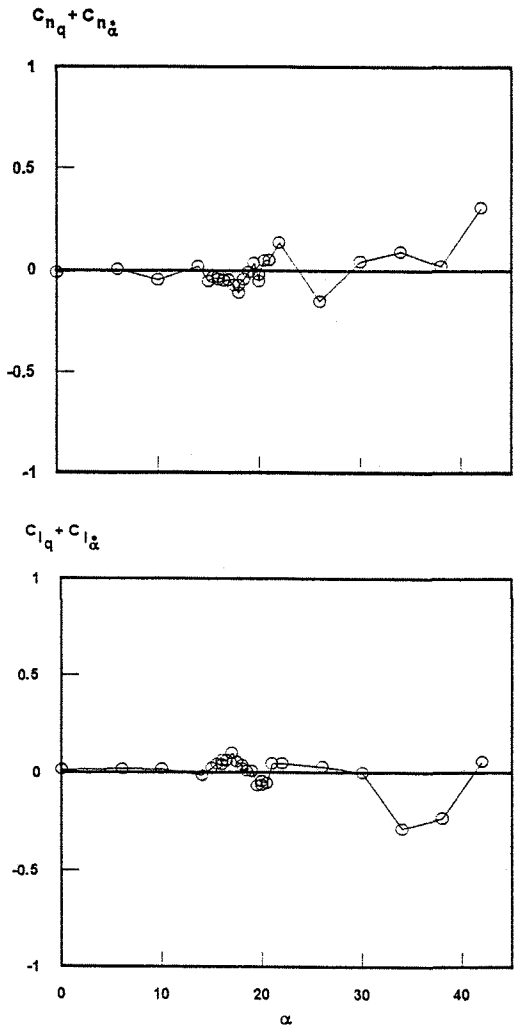

Fig 12. Cross-coupling derivatives due to q + α

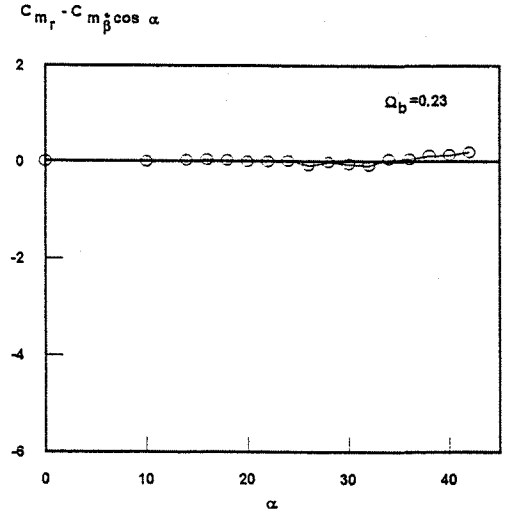

Fig 13. Cross-coupling derivatives C_{mr}-$C_{m\dot{\beta}}$cosα

derivative ($C_{lp} + C_{l\dot{\beta}} \sin \alpha$). When pitching at high angle-of-attack, the development of asymmetric flow separations on the wings will be a major contributor to ($C_{lq} + C_{l\dot{\alpha}}$). Increases in the other two derivatives are less significant.

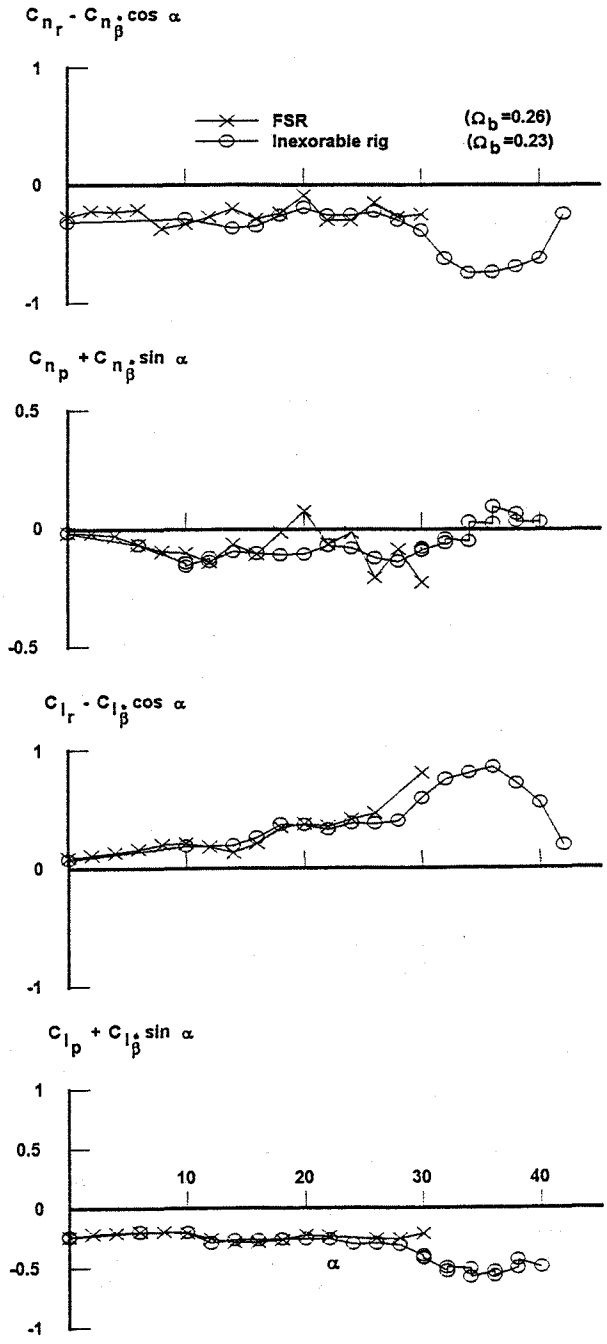

Fig 14. Comparison of results from FSR and Inexorable Rig

Comparison with results from FSR tests

Measurements of yawing and rolling moment derivatives are compared, in Fig. 14, with similar data from tests with the Flexible Sting Rig.

The latter tests were made with a conventional (heavy) model of identical geometry. In general there is good agreement between the results up to $\alpha = 30°$, the maximum test angle-of-attack for the FSR tests. Greater scatter is apparent in the FSR data.

Conclusions

A five degree-of-freedom Inexorable Rig has been designed and manufactured to measure all the significant longitudinal, lateral and cross-coupling derivatives of complete aircraft models in a low speed wind tunnel. Tests were made on a canard-configured agile fighter configuration at angles-of-attack up to 42° and results presented include the effects of frequency and model configuration on the 'static', rotary and acceleration derivatives.

The model was oscillated in five degrees-of-freedom and results showed the following:

1. There was good correlation between independent measurements of derivatives due to $\dot{\alpha}$ and $\dot{\beta}$ and combined rotary derivatives. The $\dot{\alpha}$ and $\dot{\beta}$ derivatives increased markedly for $\alpha > 25°$ and there were marked frequency and configuration effects.

2. Cross-coupling derivatives were small for $\alpha < 25°$ but the derivative $(C_{lq} + C_{l\dot{\alpha}})$ was more significant at higher angle-of-attack.

3. There was good agreement with results from tests with the Flexible Sting Rig.

The magnitudes of derivatives due to $\dot{\alpha}$ and $\dot{\beta}$ increases markedly at high angles-of-attack and serious consideration should be given to their inclusion in mathematical models and simulations of combat aircraft.

References

1 C.O. O'Leary
Dynamic tests on a High Incidence Research Model (HIRM) in a low speed wind tunnel.
RAE TR 84111, 1984

2 A.J. Ross, G.F. Edwards
Correlation of predicted and free-flight responses near departure conditions of a high incidence research model.
AGARD-CP-386, 1985

3 C.O. O'Leary
Wind-tunnel measurement of aerodynamic derivatives using flexible sting rigs. AGARD-LS-114,1981

4 C.O. O'Leary, B. Weir
Measurement of derivatives due to acceleration in heave and sideslip.
AGARD-CP-497, 1991

5 J.H. Lichtenstein, J.L. Williams
Effect of frequency of sideslipping motion on the lateral stability derivatives of a typical delta-wing airplane.
NACA RM L57F07, 1957

6 Sue B. Grafton, Ernie L. Anglin
Dynamic stability derivatives at angles of attack from -5° to 90° for a variable sweep fighter configuration with twin vertical tails.
NASA TN D-6909, 1972

7 C.O. O'Leary
Wind-tunnel measurement of lateral aerodynamic derivatives using a new oscillatory rig, with results and comparisons for the Gnat aircraft.3
ARC R&M No. 3847